

# STRUCTURAL AND PASSIVATING PROPERTIES OF SiN<sub>x</sub>:H DEPOSITED USING DIFFERENT PRECURSOR GASES

A. W. Weeber, H.C. Rieffe, W.C. Sinke, W.J. Soppe  
ECN Solar Energy, P.O. Box 1, NL-1755 ZG Petten, The Netherlands  
Phone: +31 224 564113; Fax: +31 224 568214; email: weeber@ecn.nl

**ABSTRACT:** Structural properties of SiN<sub>x</sub>:H layers deposited with N<sub>2</sub>+SiH<sub>4</sub> or NH<sub>3</sub>+SiH<sub>4</sub> using a MicroWave PECVD system are examined in detail and related to passivating properties. It is shown that the Si-N bond density is an important parameter for both surface and bulk passivation. The lower the Si-N bond density the better the surface passivation. This corresponds to higher Si-H bond densities and a higher refractive index. For maximum bulk passivation there seems to be an optimal Si-N bond density around  $1.1 \times 10^{23} \text{ cm}^{-3}$ . The Si-N bond density is related to the relative change in H content during anneal.

**Keywords:** silicon nitride, bulk passivation, surface passivation

## 1. INTRODUCTION

Recombination losses at the surface and in the bulk need to be minimized to obtain high efficiencies on multicrystalline silicon (mc-Si) solar cells. This can be achieved by using SiN<sub>x</sub>:H (hydrogenated silicon nitride) as a passivating layer. SiN<sub>x</sub>:H can passivate the surface and the bulk of the material, and can serve as an anti-reflection coating.

Passivating SiN<sub>x</sub>:H layers can be deposited using Plasma Enhanced Chemical Vapour Deposition (PECVD) techniques using nitrogen and silicon containing precursor gases. As a silicon containing precursor gas SiH<sub>4</sub> or a non-explosive diluted SiH<sub>4</sub> mixture can be used. As nitrogen containing gases NH<sub>3</sub> or N<sub>2</sub> can be used. Rieffe et al [1] and Weeber et al [2] showed that N<sub>2</sub> and SiH<sub>4</sub> as precursor gases in a MicroWave PECVD system result in excellent and thermally stable surface passivation. The bulk passivating properties for layers deposited with N<sub>2</sub> and SiH<sub>4</sub> are the same as for NH<sub>3</sub> and SiH<sub>4</sub>. The only difference is that the absorption at lower wavelengths is higher in layers deposited with N<sub>2</sub> and SiH<sub>4</sub>. Similar results were found by Hong et al [3] using an expanding thermal plasma.

In other studies excellent surface passivation for layers deposited with gas mixtures containing N<sub>2</sub>+SiH<sub>4</sub> was obtained. Schmidt and Kerr [4] found effective surface recombination velocities  $S_{\text{eff}} < 10 \text{ cm/s}$  for layers deposited using NH<sub>3</sub>/N<sub>2</sub>/SiH<sub>4</sub> gas mixtures with N<sub>2</sub> as the most abundant precursor gas. Mäckel and Lüdemann [5] analyzed the passivating properties of layers deposited using N<sub>2</sub>/H<sub>2</sub>/SiH<sub>4</sub> mixtures. The best  $S_{\text{eff}}$  values they obtained are below 10 cm/s.

In this study we investigated structural and passivating properties of SiN<sub>x</sub>:H layers deposited in an in-line MicroWave Remote Plasma Enhanced Chemical Vapour Deposition (MW RPECVD) system to obtain more information on the passivation mechanism. We used both N<sub>2</sub>/SiH<sub>4</sub> and NH<sub>3</sub>/SiH<sub>4</sub> gas mixtures for depositions.

## 2. EXPERIMENTAL

SiN<sub>x</sub>:H layers were deposited using the in-line MW RPECVD system at ECN. This system was developed in close cooperation with Roth&Rau and described in more detail in a previous paper [6]. PECVD process variables were the gas composition; pressure and gas flow.

Optical properties of the deposited layers were determined with a Filmetrics reflectometer.

The surface passivation of SiN<sub>x</sub>:H layers was determined by depositing these layers on both sides of p-type FZ Si wafers (1-2 Ωcm p type). The lifetime was measured using the Quasi Steady State Photo Conductance method [7]. To determine the thermal stability of the surface passivating properties of the layers, the lifetimes were measured before and after a thermal anneal corresponding to the firing of the metallization. Bond densities were determined using Fourier Transform Infrared (FTIR) spectroscopy combined with the analysis as reported by Bustarrett [8] and Giorgis et al [9]. The bond densities were measured before and after thermal anneals at 800 C in air for 5 to 60 minutes. For these well defined anneals an RTP furnace was used.

For a good comparison of the bulk passivating properties of the different SiN<sub>x</sub>:H layers, two groups of multicrystalline solar cells were made using neighbouring wafers (adjacent wafers from the ingot): one group with SiN<sub>x</sub>:H deposited using N<sub>2</sub>+SiH<sub>4</sub> and one using NH<sub>3</sub>+SiH<sub>4</sub>. In order to determine possible differences in passivation we fabricated complete solar cells with SiN<sub>x</sub>:H Ar coating, using in-line firing of screen printed metallization.

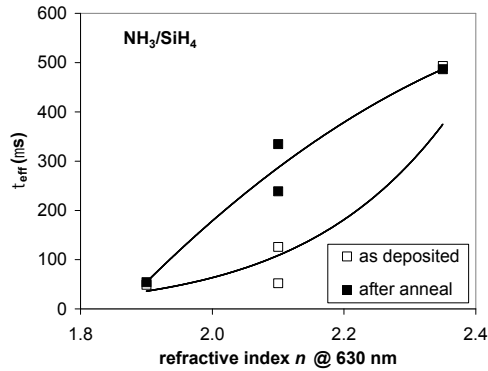
Current-voltage (IV) measurements were performed using the class A solar simulator at ECN (two current probes per busbar). Internal Quantum Efficiencies (IQE) were calculated from measured spectral responses and reflectances.

## 3. RESULTS AND DISCUSSION

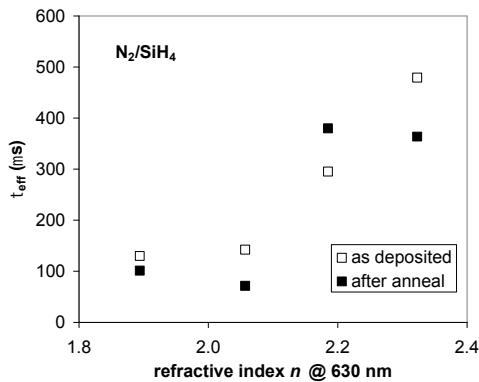
### 3.1 Bulk and surface passivation

Figure 1 and Figure 2 summarize the surface passivating properties for layers deposited with N<sub>2</sub>+SiH<sub>4</sub> or NH<sub>3</sub>+SiH<sub>4</sub>. The dependence on refractive index  $n$  is similar for both types of layers. A higher  $n$  results in a higher lifetime  $\tau_{\text{eff}}$ , and thus a better surface passivation since  $\tau_{\text{bulk}}$  will be the same for all samples. In Figure 3 the IQEs for a neighboring cells with the different SiN<sub>x</sub>:H layers are compared. It shows that the induced bulk passivation is the same for both types of layers since the IQE is the same in the wavelength region between 700 and 900 nm. The difference at shorter wavelengths can be

explained by the difference in absorption at those wavelengths.



**Figure 1:** Effective lifetime of charge carriers in FZ wafers coated with SiN<sub>x</sub>:H layers grown with NH<sub>3</sub> as precursor gas.



**Figure 2:** Effective lifetime of charge carriers in FZ wafers coated with SiN<sub>x</sub>:H layers grown with N<sub>2</sub> as precursor gas.

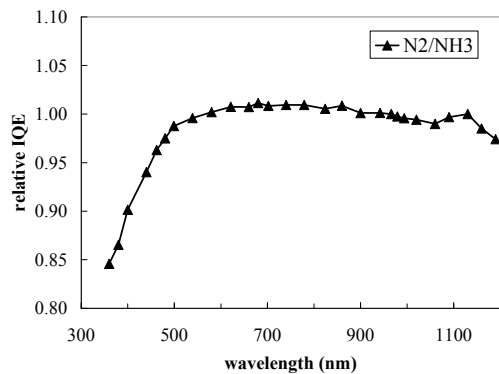


**Figure 3:** IQE ratio of two mc-Si cells with SiN<sub>x</sub>:H coatings grown with respectively N<sub>2</sub> and NH<sub>3</sub>.

### 3.2 Structural properties in relation to passivation

The Si-N bond density was determined from the IR vibrational modes between 600 and 1200 cm<sup>-1</sup>. The hydrogen bond density was calculated by peak fitting of Si-H stretch modes between 2050 and 2300 cm<sup>-1</sup> and of N-H stretch modes at 3340 cm<sup>-1</sup>. Figure 4 shows the Si-N

and Si-H bond density against *n* for layers deposited with N<sub>2</sub>+SiH<sub>4</sub>. The same densities for the ECN baseline SiN<sub>x</sub>:H deposited with NH<sub>3</sub>+SiH<sub>4</sub> are also presented. It can be seen that the Si-N bond density decreases with increasing *n* and that of Si-H increases with *n*. This is expected because SiN<sub>x</sub>:H layers with higher *n* become Si richer, and this will result in a lower Si-N bond density and a higher Si-H density. Although the ECN baseline SiN<sub>x</sub>:H layer is deposited with NH<sub>3</sub>+SiH<sub>4</sub> the bond densities correspond to those of layers deposited with N<sub>2</sub>+SiH<sub>4</sub>.

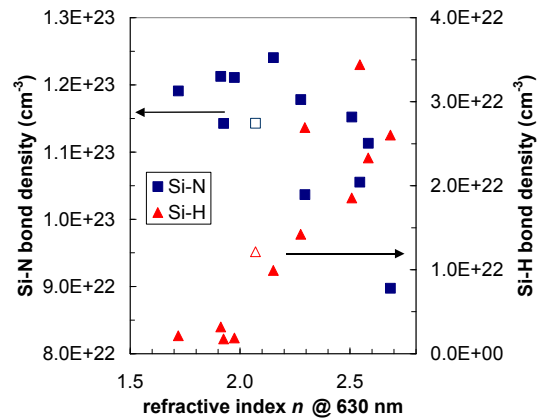


**Figure 4:** Si-N and Si-H bond densities versus the refractive index of SiN<sub>x</sub>:H layers grown with N<sub>2</sub> (filled symbols) or NH<sub>3</sub> (open symbols).

We will now discuss the effect of structural properties on the surface passivation. Figure 5 shows that for SiN<sub>x</sub>:H layers deposited with N<sub>2</sub>+SiH<sub>4</sub> the Si-H peak position is related to the lifetime measured for as-deposited layers (the higher the lifetime the better the passivation). The Si-H stretch mode peak position for the ECN baseline layer deposited with NH<sub>3</sub>+SiH<sub>4</sub> is also presented. It can be seen that for peak positions at lower wavenumbers, the passivation is better. This peak position is determined by the so-called Si-H back bonding. The peak position is at 2005 cm<sup>-1</sup> for Si<sub>3</sub>Si-H bonding and increases to 2220 cm<sup>-1</sup> for N<sub>3</sub>Si-H bonding [9]. This means for peak positions at lower wavenumbers there will be more Si back bonding, and thus *n* will be higher, which corresponds to the data summarized in Figure 4.

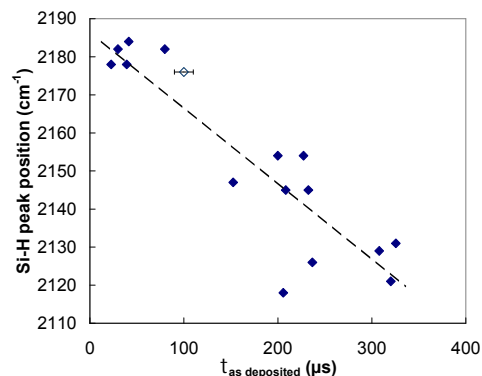


**Figure 5:** Relation between surface passivation of FZ wafers and Si-H stretch mode peak position (Filled symbols: N<sub>2</sub>, open symbol: NH<sub>3</sub> as precursor gas).

Corresponding relations can be seen between the surface passivation and the Si-N and Si-H bond density as plotted in Figure 6. Lower Si-N bond densities and higher Si-H densities result in better passivation. The lower Si-N bond density corresponds to a higher  $n$ , and thus a Si rich layer and a better surface passivation.

The results described above are comparable to those observed by Mäckel and Lüdemann [5] for a capacitive RF PECVD system using  $N_2/SiH_4/H_2$  as precursor gases. They found lower Si-N bond densities and higher Si-H densities for Si richer layers. They also found similar dependence of the lifetime (surface passivation) on the bond densities.

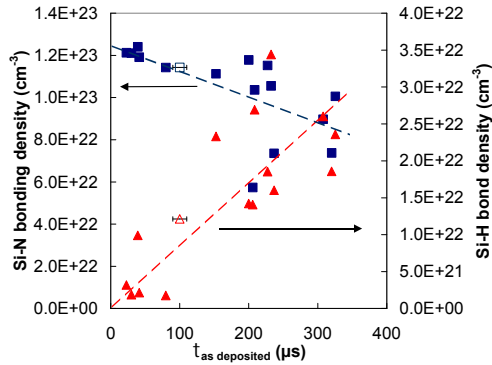


**Figure 6:** Relation between Si-N and Si-H bond densities and surface passivation by  $SiN_x:H$  layers grown with  $N_2$  (filled symbols) or  $NH_3$  (open symbols).

For bulk passivation properties the diffusion of H in the  $SiN_x:H$  layers is important. This was investigated with annealing experiments. Figure 7 shows the effects of a thermal anneal on the Si-H peak position. After 5 minutes annealing the Si-H peak position is at 2170-2180  $cm^{-1}$  for all layers, while the initial position is between 2120 and 2180  $cm^{-1}$ . This means that after an anneal the Si-H back bonding will be the same for all layers deposited in this experiment. A peak position of 2175  $cm^{-1}$  corresponds to a  $N_2Si-H_2$  bonding [9].

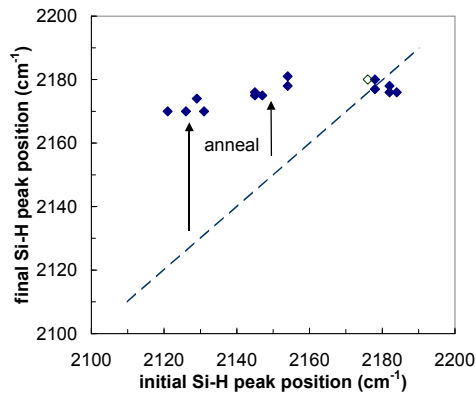


**Figure 7:** Shift of Si-H stretch mode peak position after short thermal anneal of 5 min. at 800 °C (Filled symbols:  $N_2$ , open symbol:  $NH_3$  as precursor gas).

The H fraction [H] here is defined as:

$$[H] = ([N-H] + [Si-H]) / ([N-H] + [Si-H] + [Si-N]).$$

The diffusion of H is monitored by measuring the H bond density as function of the anneal time at 800 °C. Figure 8 shows the decrease of the logarithm of the N-H bond density for a  $SiN_x:H$  layer deposited with  $N_2$  and  $SiH_4$ . The diffusion shows a strong time-dispersive (i.e. a non-linear) character that is well known for H diffusion in a-Si:H [10] and can be described by:

$$C_H = C_{H,0} \exp(-p^2 D_H t / L^2)$$

with

$$D_H(t) = D_H(0) \{\omega t\}^{-\alpha}$$

where  $\omega$  is the H attempt-to-diffuse frequency and  $\alpha$  is the temperature dependent dispersion parameter ( $0 < \alpha < 1$ ). The decrease in Si-H bond density has a similar character. It can be seen from Figure 8 that most of the H diffuses out of the layer during the first 5 minutes. Further details about this dispersive character of H diffusion in  $SiN_x:H$  can be found in [11].

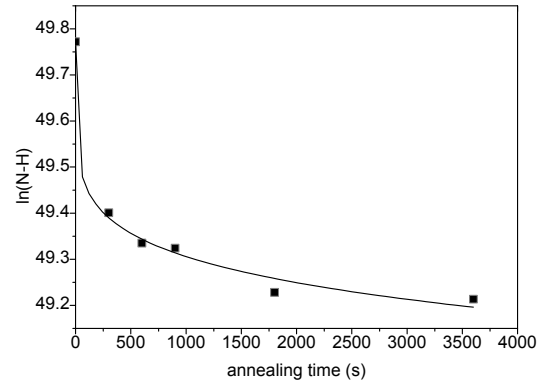


**Figure 8:** Typical example of time-dispersive behaviour of hydrogen content decrease in  $SiN_x:H$  during thermal anneal.

The degree of bulk passivation depends on the number of H atoms that will diffuse from the  $SiN_x:H$  layer into the bulk of the Si material. For  $SiN_x:H$  layers grown with MW-PECVD however, we found no relation between the initial H content and bulk passivation. IQEs above 70% are observed for all H concentrations. The initial H content for ECN baseline layer deposited with  $NH_3+SiH_4$  is also depicted.

Junegie et al. showed that the bulk passivation depends on the atomic density of the layer: the lower the density the less passivation. Van Erven et al. [12] has shown that the atomic density can be related to the Si-N bond density of the layer: higher atomic densities are found for layers with higher Si-N bond densities. Lower densities imply a more open structure that facilitates  $H_2$  formation during anneal.  $H_2$  can be considered as lost hydrogen for passivation since these molecules will not diffuse into the wafer but will evaporate into the ambient. Higher densities, however, lead to a lower hydrogen diffusion coefficient [11], probably because of deeper hydrogen traps. Figure 9 shows the IQE at 1000 nm related to the initial Si-N bond density for layers deposited with  $N_2+SiH_4$ . For layers with an Si-N bond density less than  $10^{23} cm^{-3}$  the IQEs are below 70%. For densities more than  $1.2 \cdot 10^{23} cm^{-3}$  the IQEs also are below 70%.

This could mean that the layer is too dense to obtain good bulk passivation during firing of the metallization. Maybe longer annealing times should result in better bulk passivation for those layers. This can explain why an optimum Si-N bond density is found. The Si-N bond density for the ECN baseline  $\text{SiN}_x\text{:H}$ , deposited with  $\text{NH}_3+\text{SiH}_4$  and which obtains good bulk passivation, is also presented, and is at the optimum Si-N bond density.

The relation of IQE to the final Si-N bond density is similar to that of the initial Si-N bond density, it is only shifted to higher bond densities. The Si-N density increases during the anneal by a constant value of  $1.4 \cdot 10^{22} \text{ cm}^{-3}$  for all layers. This means that the layers become denser during anneal.

Another parameter that could be important for bulk passivation, and is probably related to the density of the layer, is the relative change in H content. The IQE related to the relative change in H content for layers deposited with  $\text{N}_2+\text{SiH}_4$  is shown in Figure 10. A clear optimum between 35 and 65% can be seen. The ECN baseline  $\text{SiN}_x\text{:H}$  releases somewhat more than 20% of its H. That the relative change in H is related to the density can also be seen in Figure 11. A clear relation is visible and for layers with Si-N bond densities less than  $8 \cdot 10^{22} \text{ cm}^{-3}$  all H releases during anneal. The symbol for the ECN baseline  $\text{SiN}_x\text{:H}$  layer lies below that of the corresponding values for layers deposited with  $\text{N}_2+\text{SiH}_4$ .

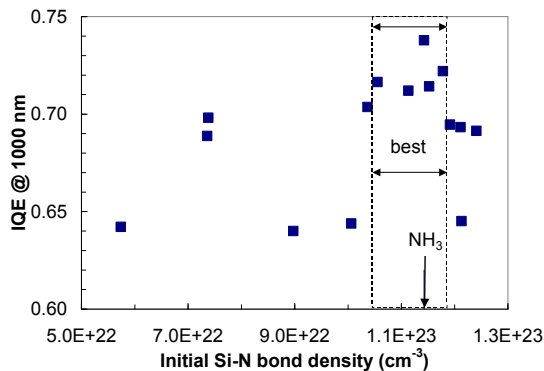


**Figure 9:** Initial Si-N bond densities in  $\text{SiN}_x\text{:H}$  layers and IQE of cells fabricated in this study.

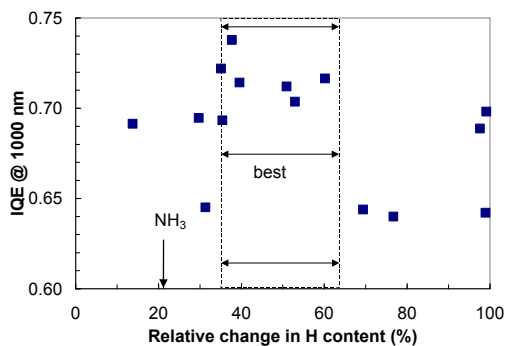


**Figure 10:** Reduction of hydrogen fractions in  $\text{SiN}_x\text{:H}$  layers during anneal and IQE of cells fabricated in this study.

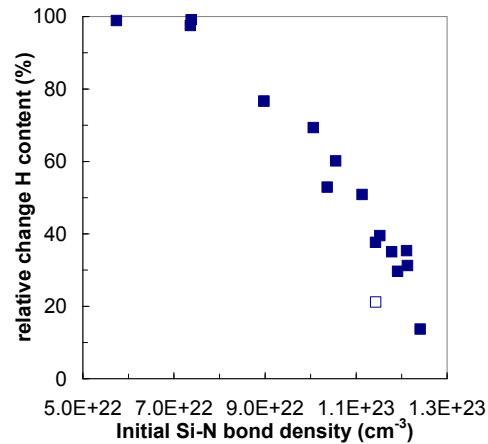


**Figure 11:** Relation between initial Si-N bond density and reduction of hydrogen content in  $\text{SiN}_x\text{:H}$  layers during anneal (Filled symbols:  $\text{N}_2$ , open symbol:  $\text{NH}_3$  as precursor gas).

#### 4 CONCLUSIONS

It is shown that the Si-N bond density is an important indicator for both surface and bulk passivation using  $\text{SiN}_x\text{:H}$  layers. The lower the Si-N bond density the better the surface passivation. This corresponds to higher Si-H bond densities and higher  $n$  values. To obtain good bulk passivation there seems to be an optimal Si-N bond density around  $1.1 \cdot 10^{23} \text{ cm}^{-3}$ . Good bulk passivation is related to an optimal relative change in H content during an short anneal 800 C of about 35-65 % for layers grown with  $\text{N}_2$  and of about 20 % for layers grown with  $\text{NH}_3$ .

#### ACKNOWLEDGEMENTS

This work was financially supported by NovemSenter in the DEN programme.

#### REFERENCES

- [1] H.C. Rieffe, et al. Proceedings PV in Europe from PV Technology to Energy Solutions (2002) 295.
- [2] A.W. Weeber, et al., Proceedings 3rd WCPEC (2003) 4PA881.
- [3] J. Hong, et al., J. Vac. Sci. Techn. B: 21 (2003) 2123.
- [4] J. Schmidt, M. Kerr, A. Cuevas. Semi. Sci. Techn.16 (2001) 164.
- [5] H. Mäkel, R Lüdemann. J.Appl. Phys. 92 (2002) 2602.
- [6] W.J. Soppe, et al., Proceedings 16<sup>th</sup> European Photovoltaic Solar Energy Conference, (2000)1420.
- [7] R.A. Sinton, A. Cuevas, Appl. Phys. Lett 69 (1996) 2510.
- [8] E. Bustarret, et al., Phys. Rev B 38 (1988) 8171.
- [9] F. Giorgis, et al., Phil. Mag. B 77 (1998) 925.
- [10] W. Beyer, Sol. Energy Mat. Sol Cells 78 (2003) 235.
- [11] W. Soppe, et al., to be submitted to J. Appl. Phys.
- [12] A.J.M. van Erven et al. this conference, 2CV.2.20.